CHAPTER 10

CASE STUDY BASELINE ANALYSIS RESULTS AND MODEL VERIFICATION

This chapter discusses the results from the case studies described in Section 8.6. Explanation of the assembly rating metrics shown in the analysis result tables can be found in Chapter 6. Explanation of the constraint variable names in the constraint configuration table can be found in Chapter 7. It should be noted that the geometries of these case studies, especially ones that are derived from real parts, are abstracted and simplified to reduce computational complexity and ease data interpretation. The simplification is done by eliminating features such as rounded corners, estimating curved that are closed to straight lines as such, and ignoring part shape that does not change the constraint configuration.

10.1 Exactly constrained geometry - Thompson's chair

The Thompson's chair is an imaginary three-legged stool. The foot of each leg is a sphere with first leg constrained by an inverted trihedral (CP1, CP2, CP3), the second by a V-groove (CP4, CP5), and the third by point-on-plane contact (CP6). The seventh

point constraint, CP7, is located on top of the stool. The constraint configuration is specified in Table 10.1 and Figure 10.1. The purpose of this case study is to observe and confirm the agreement between the analysis results and theoretical kinematic principles for an exactly constrained body in 3D space.
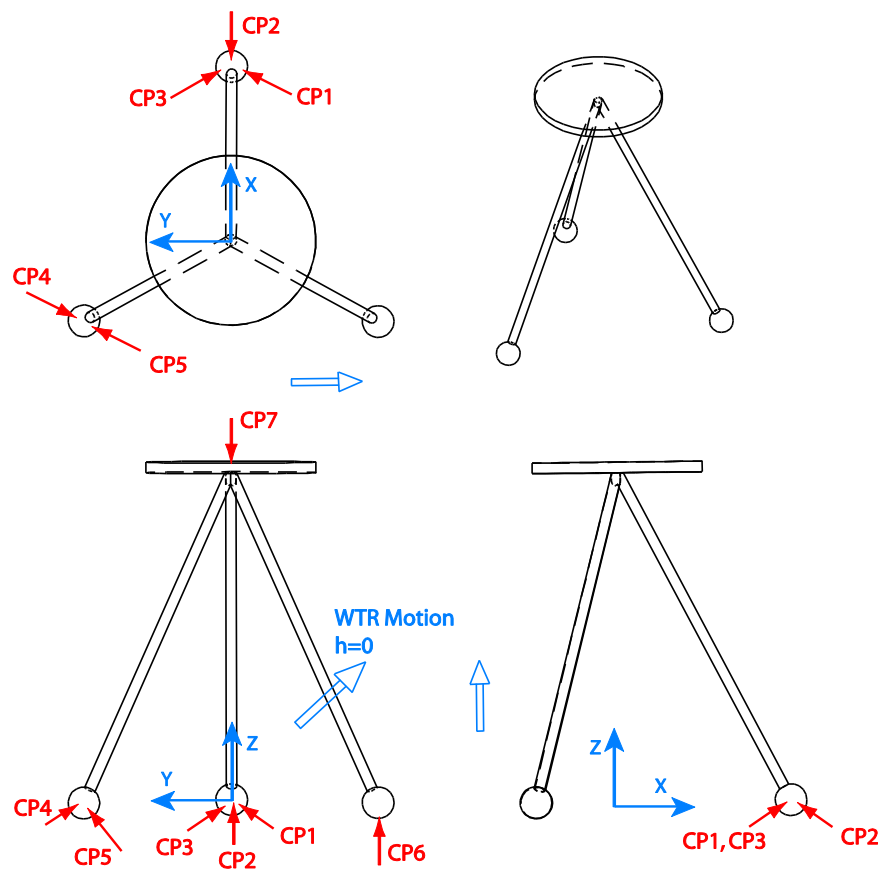

Figure 10.1 Thompson's chair constraint configuration and WTR motion

	P_x	P_y	P_z	N_x	N_y	N_z
CP1	3.570	-0.750	-0.500	0.431	0.751	0.501
CP2	4.870	0.000	-0.500	-0.867	0.000	0.498
CP3	3.570	0.750	-0.500	0.431	-0.751	0.501
CP4	-1.570	4.210	-0.500	-0.431	-0.751	0.501
CP5	-2.430	2.710	-0.500	0.431	0.751	0.501
CP6	-2.000	-3.460	-1.000	0.000	0.000	1.000
CP7	0.000	0.000	4.000	0.000	0.000	-1.000

Table 10.1 Thompson's chair constraint configuration

10.1.1 Baseline analysis results

The results are provided in Table 10.2.

Overall Rating Metric		
Weakest Total Resistance rating (WTR)	0.191	(LAR: 5.236)
Mean Redundancy Ratio (MRR)	1.000	
Mean Total Resistance Rating (MTR)	1.001	(LAR: 0.999)
Trade Off Ratio (TOR)	1.001	

	Screw axis direction (ω)			Screw axis coincident point (ρ)			Pitch (h)	Total Resistance Rating
WTR Motion 1	0.000	-0.708	0.706	-2.000	1.724	1.731	0.001	*0.191*

	Active %	Best Resistance %			Active %	Best Resistance %
CP1	14.3%	14.3%		**CP5**	14.3%	14.3%
CP2	14.3%	14.3%		**CP6**	14.3%	14.3%
CP3	14.3%	14.3%		**CP7**	14.3%	14.3%
CP4	14.3%	14.3%				

Table 10.2 Thompson's chair baseline analysis results

The WTR motion is illustrated in Figure 10.1. The WTR and MTR are relatively low compared to other case studies in this chapter. The load amplification ratio (LAR) is 5.236 (from WTR rating) and 1.001 (from MTR rating). Therefore, the reaction force of

the constraints to resist the most weakly constrained motion is about five times the input force. This is because exactly constrained assembly tends to have fewer constraints resisting the motion and hence have larger reaction forces at the support points. This is mentioned by Slocum [46] as the trade off of gaining precision of position by sacrificing load carrying capability. This trade off will be explored further in this chapter by using other case studies. The MRR is 1.000, which is expected for an exactly constrained assembly. In order to make more detailed observations, the rating matrix is provided in Table 10.3.

	CP1	CP2	CP3	CP4	CP5	CP6	CP7
Motion 1	0	0	0	0	0	0	0.329
Motion 2	0	0	0	0	0	0	0.269
Motion 3	0	0	0	0	0	0.711	0
Motion 4	0	0	0	0.829	0	0	0
Motion 5	0	0	0	0.672	0	0	0
Motion 6	0	0	0	0	0.859	0	0
Motion 7	0	0	2.871	0	0	0	0
Motion 8	0	0	1.598	0	0	0	0
Motion 9	0	0	2.078	0	0	0	0
Motion 10	0	0	0.806	0	0	0	0
Motion 11	0	2.866	0	0	0	0	0
Motion 12	0	1.595	0	0	0	0	0
Motion 13	0	0	0	0	1.381	0	0
Motion 14	0	0	0	0.401	0	0	0
Motion 15	0	0	0.747	0	0	0	0
Motion 16	0	0	0	0	0	0	0.191
Motion 17	0	0	0	0	0	0.539	0
Motion 18	1.682	0	0	0	0	0	0
Motion 19	0	0	0	1.066	0	0	0
Motion 20	0	0	0.770	0	0	0	0
Motion 21	0	0.775	0	0	0	0	0

Table 10.3 Rating matrix for Thompson's Chair (continued)

Table 10.3 Rating matrix for Thompson's Chair (continued)

Motion 22	0	0	0	0	0	0.986	0
Motion 23	0	0	0	0	0.808	0	0
Motion 24	0	0	0	0	0.712	0	0
Motion 25	0	0	0	0	0	0	0.276
Motion 26	0	0	0	0	0	0.671	0
Motion 27	0	0	0	0.859	0	0	0
Motion 28	0	0	0	0	0	0	0.640
Motion 29	0	0	0	0	0	1.068	0
Motion 30	0	0	0	0	1.391	0	0
Motion 31	0	0	0	0.539	0	0	0
Motion 32	0	0	0	0	0	0	0.634
Motion 33	0	0	0	0	0	1.058	0
Motion 34	0	2.077	0	0	0	0	0
Motion 35	0	0.604	0	0	0	0	0
Motion 36	0	0.752	0	0	0	0	0
Motion 37	0.857	0	0	0	0	0	0
Motion 38	0.806	0	0	0	0	0	0
Motion 39	0	0	0	0	1.126	0	0
Motion 40	1.593	0	0	0	0	0	0
Motion 41	0.770	0	0	0	0	0	0
Motion 42	0.770	0	0	0	0	0	0

The rating matrix shows a total of 42 evaluated motions. Because of the bi-directional nature of each screw motion, the actual number of unique pivot constraint combinations and screw motions is 21. Since each point constraint only removes a single DOF, each pivot constraint set must be composed of 5 constraint points (CP). There are 21 possible combinations in choosing 5 among the 7 constraints. In an exactly constrained geometry, each one of these pivot constraint sets needs to be a linearly independent set. This is the case for this case study because there are a total of 21 unique

combinations processed. The reciprocal motion generated by each pivot constraint set therefore is also unique.

It can be observed that for each motion (row), there are at least five constraints (for example, CP1-CP5) that are incapable of resisting the motion because they are reciprocal to it. The other remaining two constraints (CP6 and CP7) must actively resist the screw motion, or otherwise there will be unconstrained motion. It can be observed that for each motion, one of the remaining two constraints (CP6) resists the forward motion and the other (CP7) resists the backward motion. Each motion is then exactly constrained by a single active constraint, and the assembly is deterministic.

All of these observations confirm several facts summarized by Lakshminarayana [23] regarding a body constrained by seven unilateral point constraints:

- A minimum of seven unilateral point constraints is needed to achieve total restraint of a body in 3D space. If one of the constraints in this example is removed, the assembly is confirmed to lose total restraint.

- Any constraint/wrench that is linearly dependent to the pivot wrenches is unable to resist the reciprocal motion; therefore, no six of these constraints/wrenches may belong to the same linear complex; otherwise, total restraint is not achieved. When one of the constraints is modified to be linearly dependent to the set, the motion is left unconstrained, and therefore the assembly loses total restraint.

- Each motion reciprocal to five linearly independent constraints is resisted by the sixth constraint in one direction and by the seventh constraint in the other

direction. This is confirmed by the fact that only one constraint is active for each motion.

- The body constrained by seven linearly independent constraints is deterministic, namely that the actual reaction force can be found with a static equilibrium analysis because only one constraint can resist the motion.

A histogram for the total resistance for each motion is shown in Figure 10.2. The total resistance histogram is useful to observe how the most weakly constrained motions are rated relative to the rest of the evaluated motions. In this case, the motion total resistance has a relatively wide spread. Some motions are rated very strongly, while others are rated close to the average total resistance (MTR) of 1.001.
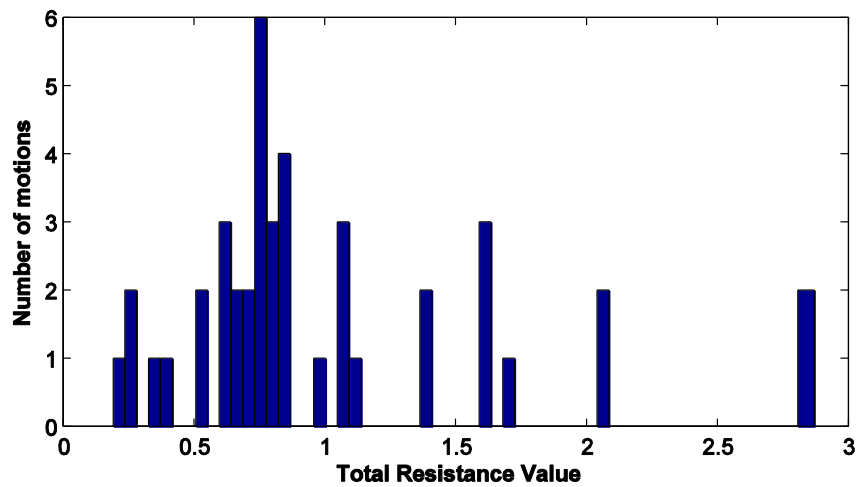

Figure 10.2 Thompson's chair total resistance histogram

10.2 Simple 3D shape geometry - generic cube

The generic cube is a 1"x1"x1" cube with point constraints on all its faces at various locations (Figure 10.3). The purpose of this geometry is to observe the behavior

of scalability of the constraint configuration as well as constraint addition and reduction trade-off study for a simple case. The constraint configurations for all 15 constraint points are specified in Table 10.4, and the different constraint combinations depending on the number of constraints for each particular case study are given in Table 10.5.
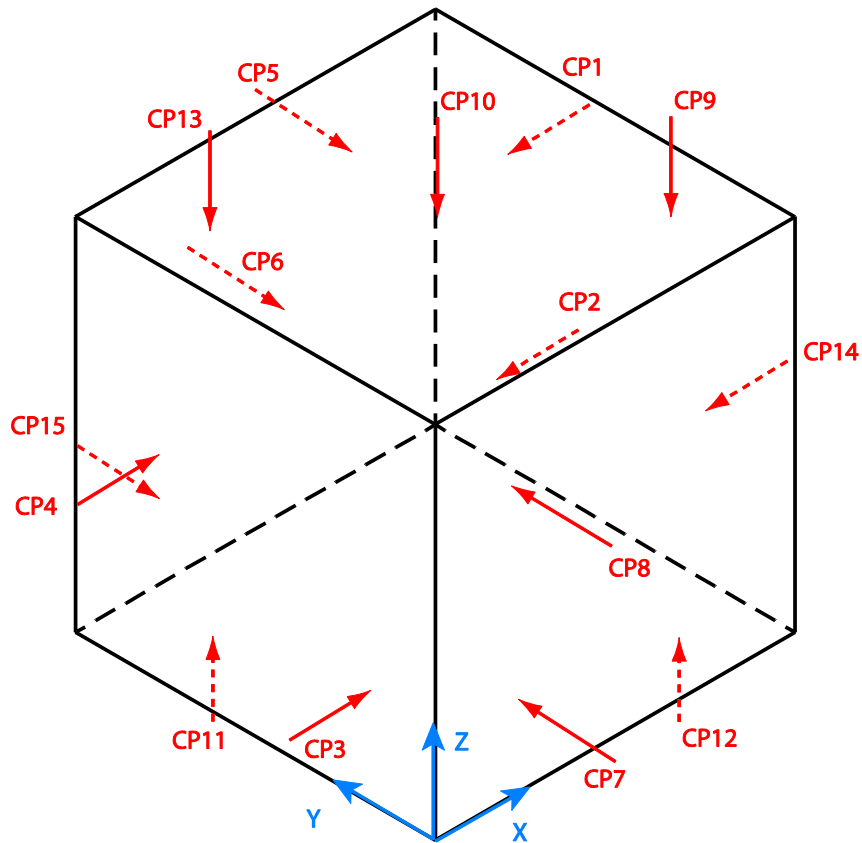

Figure 10.3 Generic cube constraint configuration

	P_x	P_y	P_z	N_x	N_y	N_z
CP1	1.000	0.750	0.750	-1.000	0.000	0.000
CP2	1.000	0.750	0.250	-1.000	0.000	0.000
CP3	0.000	0.250	0.250	1.000	0.000	0.000
CP4	0.000	0.750	0.500	1.000	0.000	0.000
CP5	0.750	1.000	0.750	0.000	-1.000	0.000
CP6	0.500	1.000	0.500	0.000	-1.000	0.000
CP7	0.250	0.000	0.250	0.000	1.000	0.000
CP8	0.250	0.000	0.750	0.000	1.000	0.000
CP9	0.750	0.250	1.000	0.000	0.000	-1.000
CP10	0.500	0.500	1.000	0.000	0.000	-1.000
CP11	0.250	0.750	0.000	0.000	0.000	1.000
CP12	0.750	0.250	0.000	0.000	0.000	1.000
CP13	0.250	0.750	1.000	0.000	0.000	-1.000
CP14	1.000	0.250	0.500	-1.000	0.000	0.000
CP15	0.250	1.000	0.250	0.000	-1.000	0.000

Table 10.4 Cube constraint configuration

Number of constraints	Constraint combination
7	CP2,CP3,CP4,CP5,CP7,CP10,CP12
8	CP1,CP2,CP3,CP4,CP5,CP7,CP10,CP12
9	CP1,CP2,CP3,CP4,CP5,CP6,CP7,CP10,CP12
10	CP1,CP2,CP3,CP4,CP5,CP7,CP8,CP10,CP11,CP12
11	CP1,CP2,CP3,CP4,CP5,CP6,CP7,CP8,CP10,CP11,CP12
12	CP1,CP2,CP3,CP4,CP5,CP6,CP7,CP8,CP9,CP10,CP11,CP12
13	CP1,CP2,CP3,CP4,CP5,CP6,CP7,CP8,CP9,CP10,CP11,CP12,CP13
14	CP1,CP2,CP3,CP4,CP5,CP6,CP7,CP8,CP9,CP10,CP11,CP12,CP13,CP14
15	CP1,CP2,CP3,CP4,CP5,CP6,CP7,CP8,CP9,CP10,CP11,CP12,CP13,CP14,CP15

Table 10.5 Cube constraint combination for different number of constraints

10.2.1 Baseline analysis results

Table 10.6 shows the baseline analysis results for the simple cube model.

Overall Rating Metric		
Weakest Total Resistance rating (WTR)	0.200	(LAR: 5.003)
Mean Redundancy Ratio (MRR)	1.000	
Mean Total Resistance Rating (MTR)	0.486	(LAR: 2.057)
Trade Off Ratio (TOR)	0.486	

	Screw axis direction (ω)			Screw axis coincident point (ρ)			Pitch (h)	Total Resistance Rating
WTR Motion 1	0.577	-0.577	0.577	0.333	0.750	0.417	0.083	*0.200*
WTR Motion 2	0.667	-0.667	-0.333	0.694	0.417	0.556	-0.222	*0.216*

	Active %	Best Resistance %			Active %	Best Resistance %
CP1	14.3%	14.3%		CP5	14.3%	14.3%
CP2	14.3%	14.3%		CP6	14.3%	14.3%
CP3	14.3%	14.3%		CP7	14.3%	14.3%
CP4	14.3%	14.3%				

Table 10.6 Cube baseline analysis result (7 constraints)

The number of pivot constraint combinations that form a linearly dependent set is significantly higher. For the 15 constraints case, only 2.1% of the possible 4823 pivot constraint sets yield unique screw motions. This is due to the parallel and collinear nature of the relative positions and orientations of the constraints. The algorithm improves the efficiency of the analysis tool by recognizing these duplicate motions as well as the linear dependence between constraints. The overall computational improvement in this case is about one to two orders of magnitude, assuming the same amount of computation time for each iteration.

10.2.2 Scalability test case study

The purpose of this case study is to compare the analysis results between the baseline geometry and the scaled geometry. The issue of scalability was discussed in Section 3.4. The isolated reaction force couple model should resolve the scalability issues as well as the discontinuity between rotation and translation scaling that occur in other models. A scale factor of 2 is applied to the cube, and the comparison between the baseline model and the scaled model is shown in Table 10.7.

	Cube (Scale=1)	Cube (Scale=2)	% Difference
WTR	0.200	0.189	-5%
MRR	1.000	1.000	0%
MTR	0.486	0.473	-3%
TOR	0.486	0.473	-3%

Table 10.7 Cube scalability test result comparison

It can be observed that the results differ by 3-5% on average. The small difference is due to the shift in screw motion with finite pitches. Table 10.8 shows the comparison between the pitch of each motion and its associated total resistance value.

	h1	h2	h2/h1		h1	h2	h2/h1
Motion 1	Inf	Inf	-	**Motion 22**	Inf	Inf	-
Motion 2	0.000	0.000	-	**Motion 23**	0.000	0.000	-
Motion 3	0.000	0.000	-	**Motion 24**	0.000	0.000	-
Motion 4	0.000	0.000	-	**Motion 25**	0.000	0.000	-
Motion 5	0.000	0.000	-	**Motion 26**	0.000	0.000	-
Motion 6	Inf	Inf	-	**Motion 27**	Inf	Inf	-
Motion 7	0.000	0.000	-	**Motion 28**	0.000	0.000	-
Motion 8	0.000	0.000	-	**Motion 29**	0.000	0.000	-
Motion 9	-0.250	-0.500	**2.000**	**Motion 30**	-0.250	-0.500	**2.000**
Motion 10	0.000	0.000	-	**Motion 31**	0.000	0.000	-
Motion 11	0.125	0.250	**2.001**	**Motion 32**	0.125	0.250	**2.001**
Motion 12	0.250	0.500	**2.000**	**Motion 33**	0.250	0.500	**2.000**
Motion 13	0.000	0.000	-	**Motion 34**	0.000	0.000	-
Motion 14	0.000	0.000	-	**Motion 35**	0.000	0.000	-
Motion 15	0.000	0.000	-	**Motion 36**	0.000	0.000	-
Motion 16	0.042	0.083	**1.998**	**Motion 37**	0.042	0.083	**1.998**
Motion 17	0.167	0.333	**1.999**	**Motion 38**	0.167	0.333	**1.999**
Motion 18	-0.222	-0.445	**2.001**	**Motion 39**	-0.222	-0.445	**2.001**
Motion 19	0.111	0.222	**2.000**	**Motion 40**	0.111	0.222	**2.000**
Motion 20	-0.167	-0.333	**1.999**	**Motion 41**	-0.167	-0.333	**1.999**
Motion 21	0.083	0.167	**2.001**	**Motion 42**	0.083	0.167	**2.001**

Table 10.8 Cube scalability test – motion pitch comparison

It can be observed that for motions with zero or infinite pitch, the total resistance for the motion is identical. The reason that the resistance values are identical for zero-pitch motions (pure rotation) is as follows. When the motion is a rotation-dominant, the input torque is also scaled according to the maximum distance between the screw axis and the constraint positions. This distance is scaled by 2 for the scaled model. If the input load magnitude were not changed, the scaled model would have better resistance to the motion. This is what caused the scalability issue of the previous model by Bausch [7] and Bozzo [9]. By modeling the input load as a force couple with a properly scaled input

moment arm, the resistance value stays constant for the pure rotation motions. In the case of infinite pitch motions (pure translation), the total resistance stays constant because the resistance value for pure translation in this case depends only on the orientations of the constraints and not their positions. The orientations of the constraints do not change due to the scaling.

The difference in total resistance values then, occurs in the case where the pitch of the motion is non-zero and finite. This difference is caused by a difference in the motion pitch. The following is an explanation of the motion change. The motion change due to the scaling can be explained by understanding the change in the motion's screw geometry as the part geometry is scaled. Recall that each motion is reciprocal to a set of pivot constraints. The motion's virtual displacement at each of the pivot constraints location 'slides' perpendicularly with respect to each pivot constraint's normal. When the cube is scaled, the pivot constraints' relative distances from the origin and from each other are scaled. However, the motion must remain reciprocal to the set. Therefore, the motion reciprocal to the scaled pivot constraint locations also changes. The rotational component's virtual displacement at the pivot constraints is proportional to $\vec{\omega} \times \vec{R}$. Since the distrance $\vec{R}$ is scaled by 2, the rotational component's virtual displacement is also scaled by 2. This is not true for the translational component. Since the translational component of the virtual displacement is proportional to $h\vec{\omega}$, the scaling of the part size does not change the magnitude of the translational component. In order to maintain reciprocity, the translational component of the screw motion must be scaled by 2. This is

manifested in the pitch h being scaled by 2. Hence, the scaled motion reciprocal to the scaled pivot constraint location has a pitch multiplied by the scaling factor.

It can be observed in Table 10.8 that for finite-pitch motions, the motion pitch for the scaled model is twice that of the motion pitch for the base model. This is equal to the scale factor, which is two, except for rounding errors in the computation. Because the motion is not exactly identical, the resistance values to these kinds of motion are not the same.

Although the total resistance rating is slightly different for finite pitch motions, the difference in assembly rating is minimal (3-5%). In addition, a comparison between the total resistance histograms of the cube with scale factors of 1 and 2 shows that there is no noticeable difference in pattern of the motion resistance ratings (Figure 10.4 and Figure 10.5).
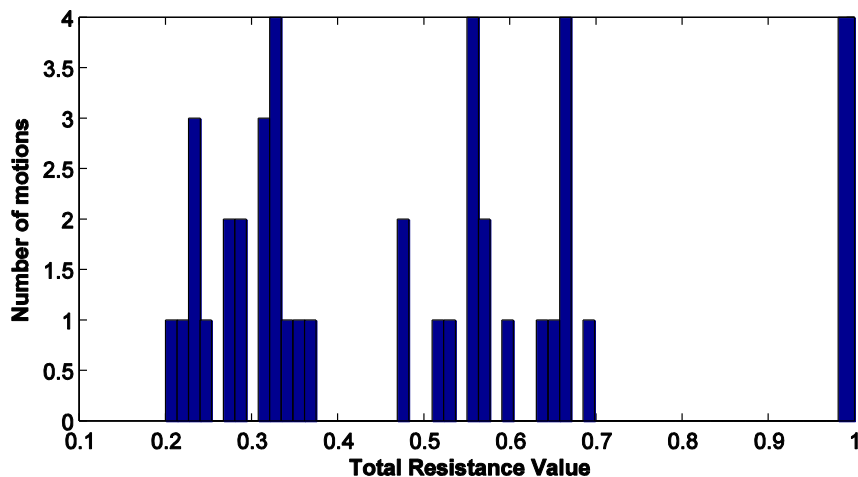

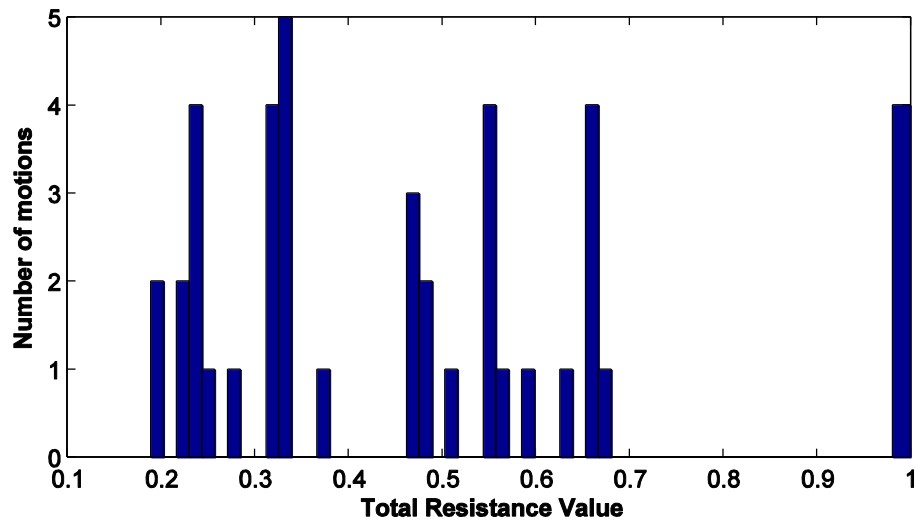**Figure 10.4 Total resistance histogramn for cube (scale factor = 1)**

166

Figure 10.5 Total resistance histogramn for cube (scale factor = 2)

In summary, the scalability test case study demonstrated that the analysis tool achieved far greater consistency and scalability compared to previous models by using the isolated reaction force couple model. The motion shift for non-zero and non-infinite pitch motions can be explained by understanding the change in the screw motion geometry, which happens when pivot constraint positions are modified.

10.3 Rectilinear geometry - battery cover assembly

The third case study is a battery cover assembly. The battery cover is assembled by inserting the two lugs at an angle, lowering the part, and engaging the two snap-fits into the mating part. The constraints are provided by two cantilever snap-fits, modeled as two point constraints, and two lugs, also modeled as two point constraints. Their length-to-overall-part-length ratio is too small to be modeled as a line constraint. There are also line constraints around the perimeter of the part and a plane constraint from the bottom of

the part. The constraint configuration of the battery cover is specified in Figure 10.6 and Table 10.9.
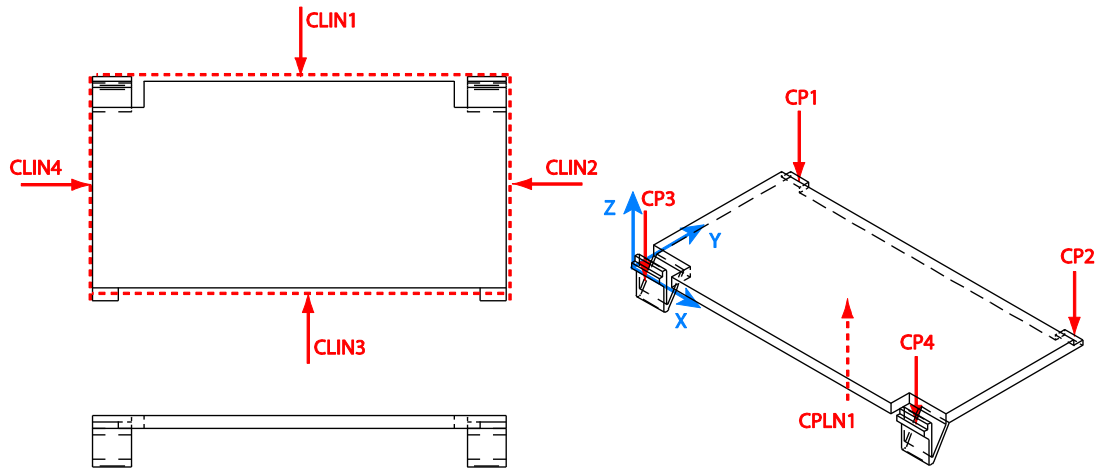

Figure 10.6 Battery cover constraint configuration

	P_x	P_y	P_z	N_x	N_y	N_z				
CP1	1	2	0	0	0	-1				
CP2	3	2	0	0	0	-1				
CP3	1	0	0	0	0	-1				
CP4	3	0	0	0	0	-1				
	P_x	P_y	P_z	w_x	w_y	w_z	N_x	N_y	N_z	L
CLIN1	0	1	0	0	1	0	1	0	0	2
CLIN2	4	1	0	0	1	0	-1	0	0	2
CLIN3	2	0	0	1	0	0	0	1	0	4
CLIN4	2	2	0	1	0	0	0	-1	0	4
	P_x	P_y	P_z	N_x	N_y	N_z	Type			
CPLN1	2	1	0	0	0	1	1			
	u_x	u_y	u_z	L_1	v_x	v_y	v_z	L_2		
CPLN_PROP1	1	0	0	4	0	1	0	2		

Table 10.9 Battery cover baseline constraint configuration

The constraint configuration in this assembly contains higher order constraints (HOC) such as line and plane constraints. The snap-fit lock is technically a line contact,

but is significantly short compared to the overall length of the part in the same direction. Therefore, it should be modeled as a point constraint. The other line contact occurs around the perimeter of the lip. Since the line contact between the lips of the battery cover and its mating part extends as long as the part length, it is obvious that this should be modeled as a line constraint. The planar constraint provided by the matic part constraints motion in the positive z direction.

10.3.1 Baseline analysis results

The baseline analysis results are shown in Table 10.10.

Overall Rating Metric		
Weakest Total Resistance rating (WTR)	2.000	(LAR: 0.500)
Mean Redundancy Ratio (MRR)	1.500	
Mean Total Resistance Rating (MTR)	2.000	(LAR: 0.500)
Trade Off Ratio (TOR)	1.333	

	Screw axis direction (ω)			Screw axis coincident point (ρ)			Pitch (h)	Total Resistance Rating
WTR Motion 1	-1.000	0.000	0.000	0.000	0.000	0.000	0.000	*2.000*
WTR Motion 2	-1.000	0.000	0.000	0.000	2.000	0.000	0.000	*2.000*
WTR Motion 3	-0.707	-0.707	0.000	0.500	-0.500	0.000	0.000	*2.000*
WTR Motion 4	-0.707	0.707	0.000	1.500	1.500	0.000	0.000	*2.000*
WTR Motion 5	0.000	-1.000	0.000	3.000	0.000	0.000	0.000	*2.000*
WTR Motion 6	0.000	-1.000	0.000	1.000	0.000	0.000	0.000	*2.000*
WTR Motion 7	-1.000	0.000	0.000	0.000	0.000	0.000	Inf	*2.000*
WTR Motion 8	0.000	-1.000	0.000	0.000	0.000	0.000	Inf	*2.000*
WTR Motion 9	0.000	1.000	0.000	0.000	0.000	0.000	Inf	*2.000*
WTR Motion 10	1.000	0.000	0.000	0.000	0.000	0.000	Inf	*2.000*
WTR Motion 11	0.000	1.000	0.000	1.000	0.000	0.000	0.000	*2.000*
WTR Motion 12	0.000	1.000	0.000	3.000	0.000	0.000	0.000	*2.000*
WTR Motion 13	0.707	-0.707	0.000	1.500	1.500	0.000	0.000	*2.000*
WTR Motion 14	0.707	0.707	0.000	0.500	-0.500	0.000	0.000	*2.000*
WTR Motion 15	1.000	0.000	0.000	0.000	2.000	0.000	0.000	*2.000*
WTR Motion 16	1.000	0.000	0.000	0.000	0.000	0.000	0.000	*2.000*

	Active %	Best Resistance %
CP1	9.4%	6.3%
CP2	9.4%	3.1%
CP3	9.4%	3.1%
CP4	9.4%	0.0%

	Active %	Best Resistance %
CLIN1	3.1%	3.1%
CLIN2	3.1%	3.1%
CLIN3	3.1%	3.1%
CLIN4	3.1%	3.1%
CPLN1	31.3%	25.0%

Table 10.10 Battery cover baseline analysis result

The analysis results for this geometry yield a very uniform rating for most of the motions. The most weakly constrained motions are 16 different but equally rated motions. In fact, they are the complete set of evaluated motions. It can also be observed that all of the motions are zero or infinite-pitch. These refer to pure rotation or pure translation motion. A comparison between the analysis results of various geometries shows that when all constraints are located in a single plane, though their orientation is three dimensional in nature, all of the evaluated motions consist exclusively of zero or infinite-pitch motions.

The plane contact is shown to be significantly more active in resisting motion as well as being the most important reaction constraint. This is typical of higher order constraints (HOC). The possibility of an HOC to resist arbitrary motion is higher because they remove more DOF. The WTR motion set shows much symmetry. There are two types of symmetry that can be observed. The first type is symmetry in the screw axis direction $\vec{\omega}$ and $-\vec{\omega}$. For example, WTR motion 1 and 16 are symmetrical in this way. The second type is symmetry in the location of the screw axis $\vec{\rho}$ with respect to the part geometry's line of symmetry. For example, WTR motion 1 and 2 are symmetrical with respect to the part line of symmetry in the x direction. These occurrences are expected for a part with a symmetrical constraint configuration.
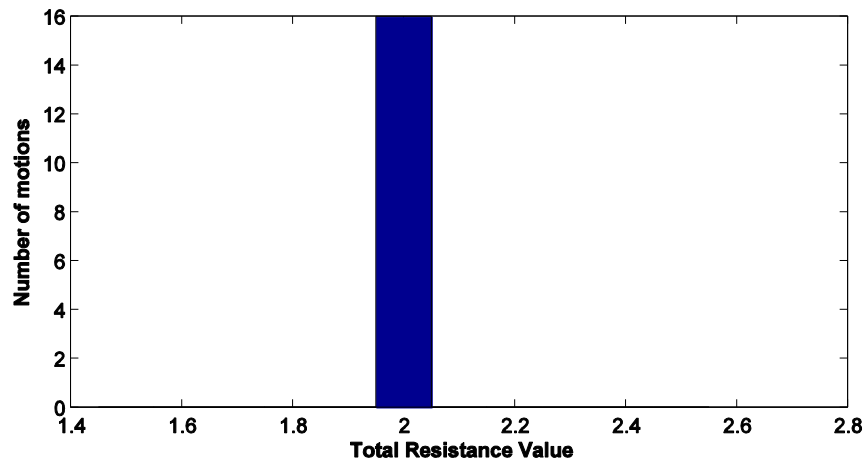
Figure 10.7 Total resistance histogram for battery cover

The total resistance histogram shows a single set of motions with a total resistance of 2.000 (Figure 10.7). The uniform rating for this case study is mainly due to the fact that almost all of the constraints are located at the edges of the part. It is common for zero and infinite pitch screw axes to pass through constraint points or be coincident with constraint directions. In these cases, the input wrench force couple moment arm is equal to the moment arm of the resisting constraints, yielding a resistance value of 1. When there are two constraints involved in this case, the total resistance rating becomes 2.

Assembly with a histogram that is very narrow tends to have very uniform strength in many different directions. In a way, it is stronger to resist more arbitrary loads compared to assembly with a wider spread in the total resistance histogram. A large deviation in the total resistance histogram implies that the assembly is stronger in some directions and weaker in others. The total resistance histogram is useful in determining the omni-directional tendency of an assembly's strength.

172

10.4 Axisymmetric geometry - end cap assembly

The axisymmetric assembly geometry is represented by the end cap assembly. The end cap is part of an assembly of a medicine spray housing. The locking feature is provided by two cantilever snap-fits located symmetrically at the lips of the end cap assembly. The part is also constrained by a pin constraint and a plane constraint, both provided by the lip mating interface. The constraint configuration of the end cap assembly is specified in Figure 10.8 and Table 10.11.
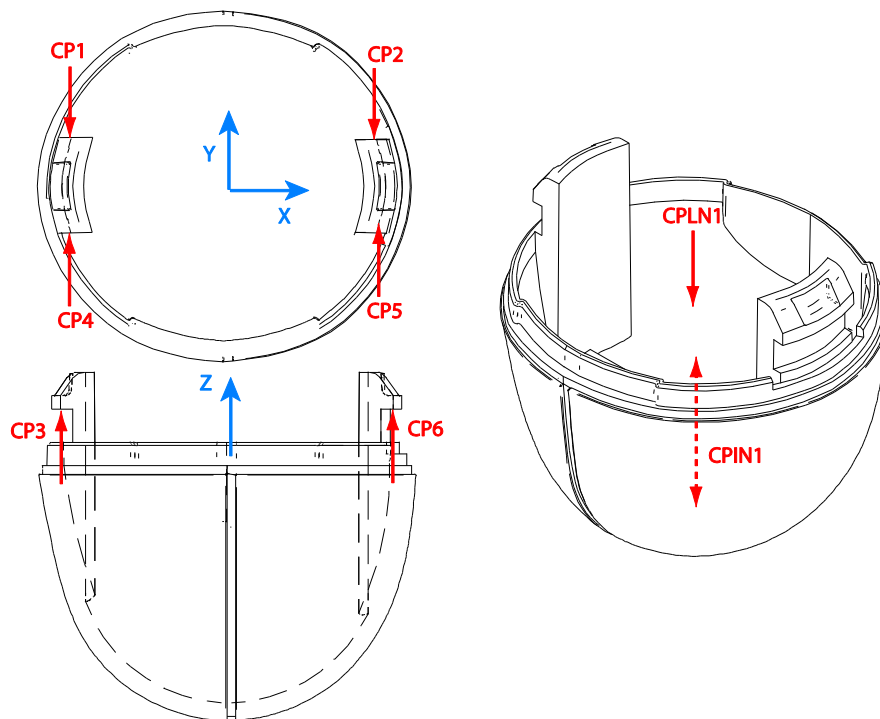

Figure 10.8 Endcap geometry and constraint configuration

	P_x	P_y	P_z	N_x	N_y	N_z	
CP1	-0.588	0.161	0.188	0.000	-1.000	0.000	
CP2	0.588	0.161	0.188	0.000	-1.000	0.000	
CP3	-0.588	0.000	0.188	0.000	0.000	1.000	
CP4	-0.588	-0.161	0.188	0.000	1.000	0.000	
CP5	0.588	-0.161	0.188	0.000	1.000	0.000	
CP6	0.588	0.000	0.188	0.000	0.000	1.000	
	P_x	P_y	P_z	w_x	w_y	w_z	
CPIN1	0.000	0.000	0.000	0.000	0.000	1.000	
	P_x	P_y	P_z	N_x	N_y	N_z	*Type*
CPLN1	0.000	0.000	0.000	0.000	0.000	-1.000	2.000
	r						
CPLN_PROP1	0.625						

Table 10.11 End cap constraint configuration

The assembly contacts that need to be considered for higher order constraint modeling in this case are the curved line contact in the z-axis direction, the curved line contact in the radial direction on the XY-plane, and the line contact between the snap-fit retention face and the mating part.

The curved line contact that constrains the end cap in the negative z-direction exhibits a circular plane constraint. Although both rectangular and circular plane constraints have an identical wrench system, it is important to note the circular shape of the plane because in the isolated reaction force model, the finite size of the plane of the reaction wrench is taken into account. The curved line contact that constrains the end cap in the radial direction exhibits a pin constraint because it eliminates translational DOF in the X and Y directions.

The line contact between the snap-fit retention face and the mating part does not extend to the overall part length, but its length is not insignificant. However, since the

wrench system that belongs to the line contact is also a subsystem of the plane contact, it is safe to model this as a point contact to allow more motions to be evaluated. In other words, if the snap-fit is modeled as a line constraint, the line constraint is linearly dependent on the plane constraint. If the line contact is modeled as a point contact, there is an additional combination of pivot constraints that adds more motions to consider. When too many HOC are added to a part, the number of motions evaluated can be reduced to a very small number. Hence, in order to take a more conservative approach, computational efficiency is sacrificed for the sake of evaluating more motions and gaining more data to understand the assembly. This limitation is discussed further in Chapter 12.

10.4.1 Baseline results

Table 10.12 shows the results of the analysis.

Overall Rating Metric		
Weakest Total Resistance rating (WTR)	1.000	(LAR: 1.000)
Mean Redundancy Ratio (MRR)	1.277	
Mean Total Resistance Rating (MTR)	1.811	(LAR: 0.552)
Trade Off Ratio (TOR)	1.418	

	Screw axis direction (ω)			Screw axis coincident point (ρ)			Pitch (h)	Total Resistance Rating
WTR Motion 1	0.000	-1.000	0.000	0.588	0.000	0.000	0.000	*1.030*
WTR Motion 2	-1.000	0.000	0.000	0.000	0.000	0.000	Inf	*1.000*
WTR Motion 3	1.000	0.000	0.000	0.000	0.000	0.000	Inf	*1.000*
WTR Motion 4	0.000	1.000	0.000	-0.588	0.000	0.000	0.000	*1.030*

	Active %	Best Resistance %			Active %	Best Resistance %
CP1	10.0%	5.0%		CPIN1	10.0%	10.0%
CP2	10.0%	5.0%				
CP3	5.0%	5.0%		CPLN1	40.0%	30.0%
CP4	10.0%	0.0%				
CP5	10.0%	0.0%				
CP6	5.0%	5.0%				

Table 10.12 End cap baseline analysis results

The baseline analysis results show that the WTR rating for the assembly is 1.000.
Similar with the battery cover geometry, most of the constraints in this assembly are
located at the edges of the parts, and therefore most of the reaction constraints have a
resistance rating of 1 or greater. The total resistance histogram (Figure 10.9) shows three
sets of motions that are rated similarly. The histogram is useful in observing that the
motions are grouped into these sets. When the WTR motion is to be increased, the

designer needs to improve the resistance to *all* of the motions that are most weakly constrained (in this case, there are 4 motions).

Similar to the battery cover, the end cap assembly exhibits symmetry in the evaluated motion set with respect to screw axis direction (WTR motion 1 and 4). Another similarity is that the evaluated motion set consists exclusively of zero and infinite-pitch motions because all of the constraints are located on a single plane.
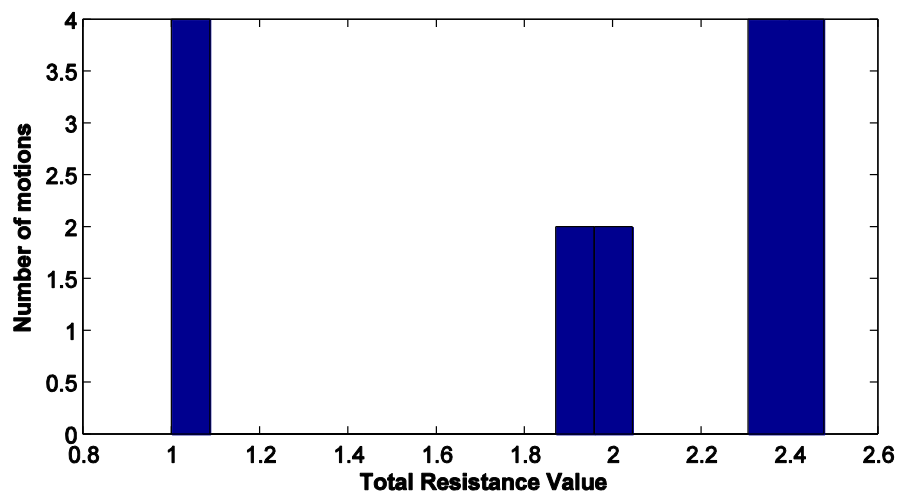

Figure 10.9 Total resistance histogram for end cap

10.4.2 HOC model vs. non-HOC model

In order to observe the computational efficiency and accuracy of the higher order constraint (HOC) modeling, a contrast between the HOC model and a non-HOC model is studied in this section. The non-HOC model discretizes the pin and plane constraints in the end cap assembly into point constraints. The pin constraint is discretized into 8 point constraints with the normal vector directed to the center of the pin. The plane constraint is

discretized into 8 parallel point constraints with the normal direction in the negative z-direction. Table 10.13 specifies the constraint configuration of this model.

	P_x	P_y	P_z	N_x	N_y	N_z
CP1	-0.588	0.161	0.000	0.000	-1.000	0.000
CP2	0.588	0.161	0.000	0.000	-1.000	0.000
CP3	-0.588	-0.161	0.000	0.000	1.000	0.000
CP4	0.588	-0.161	0.000	0.000	1.000	0.000
CP5	-0.588	0.161	0.000	0.000	0.000	1.000
CP6	0.588	0.161	0.000	0.000	0.000	1.000
CP7	-0.588	-0.161	0.000	0.000	0.000	1.000
CP8	0.588	-0.161	0.000	0.000	0.000	1.000
CP9	-0.633	0.000	0.000	0.000	0.000	-1.000
CP10	0.000	-0.633	0.000	0.000	0.000	-1.000
CP11	0.633	0.000	0.000	0.000	0.000	-1.000
CP12	0.000	0.633	0.000	0.000	0.000	-1.000
CP13	-0.448	-0.448	0.000	0.000	0.000	-1.000
CP14	0.448	-0.448	0.000	0.000	0.000	-1.000
CP15	-0.448	0.448	0.000	0.000	0.000	-1.000
CP16	0.448	0.448	0.000	0.000	0.000	-1.000
CP17	-0.633	0.000	0.000	1.000	0.000	0.000
CP18	0.000	-0.633	0.000	0.000	1.000	0.000
CP19	0.633	0.000	0.000	-1.000	0.000	0.000
CP20	0.000	0.633	0.000	0.000	-1.000	0.000
CP21	-0.448	-0.448	0.000	0.707	0.707	0.000
CP22	0.448	-0.448	0.000	-0.707	0.707	0.000
CP23	-0.448	0.448	0.000	0.707	-0.707	0.000
CP24	0.448	0.448	0.000	-0.707	-0.707	0.000

Table 10.13 End cap assembly constraint configuration (non-HOC model)
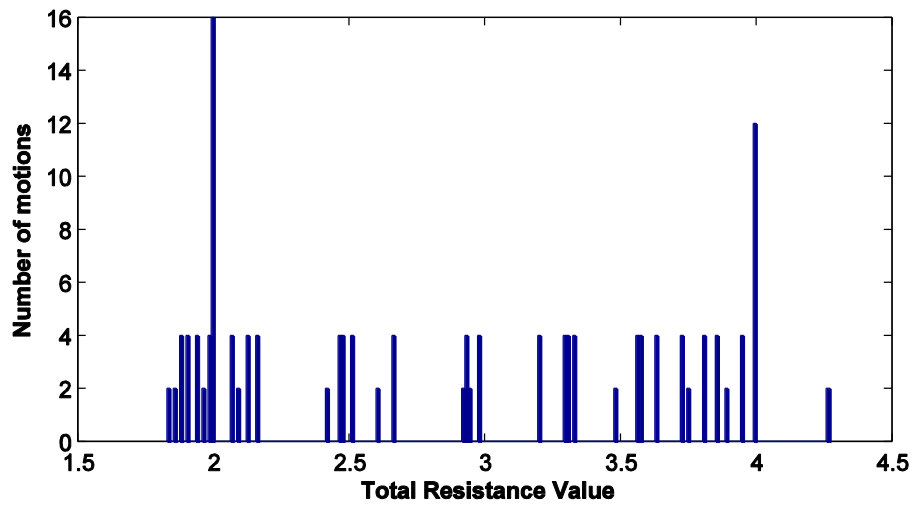
Figure 10.10 End cap total resistance histogram (non-HOC model)

	HOC model	Non-HOC model
Analysis elapsed time (sec)	0.36	12.5
Initial number of combinations	210	42504
Processed number of motion (includes duplicates due to symmetry)	20	282
Unique motion evaluated	12	148
WTR	1.000	1.829
MRR	1.277	3.028
MTR	1.811	2.855
TOR	1.418	0.943

Table 10.14 Comparison of HOC vs. non-HOC model analysis results

Table 10.14 summarizes the comparison. The computational time of the HOC model is one to two orders of magnitude less because the number of combinations the non-HOC model needs to address is much higher. The difference between the combination to begin with and the actual number of processed motions is the number of

179

pivot constraint combinations that are not linearly independent (the rank is less than 5).

Most often this is due to combining constraints that belong to the same HOC.

The analysis results show that the non-HOC model is rated higher in general compared to the HOC model. However, this higher rating is mainly due to the pseudo-redundancy effect as was previously explained in Section 3.4.1. The histogram (Figure 10.10) shows that the non-HOC model evaluates considerably more motions than the HOC model. A closer look reveals that many of these motions' pivot constraint sets contain only one or two wrenches that are taken from the HOC of which they are members. Therefore, these are 'fictitious' motions that do not actually need to be evaluated in the assembly. Many of them also tend to be rated higher because the resistance can come from other discretized point constraints. For example, one of the evaluated motions is specified in Table 10.15.

	Screw axis direction (ω)			Screw axis coincident point (ρ)			Pitch (h)
Motion	-0.269	-0.963	0.000	-0.587	0.164	0.000	0.000
Pivot constraints	CP1, CP2, CP5 CP9, CP23						
Active reaction constraints	CP10, CP11, CP12, CP13,CP14, CP15,CP16						

Table 10.15 Sample motion to illustrate pseudo-redundancy

CP9 is shown as one of the pivot constraints, and the motion is actively resisted by CP10-CP16, but CP9-CP16 belongs to the same constraint feature, namely the planar constraint around the lip of the end cap. Therefore, this motion is reciprocal to *and* actively resisted by the same constraint feature. This is inconsistent with the screw theory principle that a wrench reciprocal to a screw motion cannot do any work, or in this case, resist the

motion. This motion should not be in the evaluated motion set because it is contradictory to the screw theory principle and will skew the rating of the assembly. The high rating of the non-HOC model then is mostly due to these kinds of motions. This example illustrates the pseudo-redundancy effect. The HOC model eliminates the possibility of such combinations. Hence, it offers greater efficiency as well as greater accuracy.

As a bi-product of the efficiency, the number of evaluated motions is very few compared to the non-HOC model. Using the HOC model prevents evaluation of motions that violate the screw theory principle such as the one explained in the previous paragraph. However, when a line contact that is relatively short compared to the part length is modeled as an HOC, this reduces the amount of information. When the designer wants to be on the conservative side of the analysis, one should be less likely to use HOC modeling. The likelihood of a short line to be modeled as a line constraint instead of a point constraint is directly related to the HOC usage guideline. This guideline is needed to define the critical length when a line is long enough to be modeled as a line constraint. The same case applies for plane constraints.

10.5 Freeform/non-planar geometry - printer housing assembly

The final case study is focused on a real part where constraints are not necessarily oriented in a rectilinear fashion and the shape of the part leans toward freeform geometry. The organic/freeform shapes are popular with some branches of industrial design. This is where the design tool is most useful, namely to evaluate the possibility of exploring various design spaces that are not intuitive to the designer.

The printer housing assembly from an Epson Stylus C82 printer is simplified and used to represent this geometry. The printer housing is constrained by 4 threaded fasteners (the word fastener is used to prevent confusion with the term 'screw' in screw motion), 5 cantilever snap-fits, and line constraints along the perimeter edges of the part. The assembly constraints are specified in Figure 10.11 and Table 10.16.
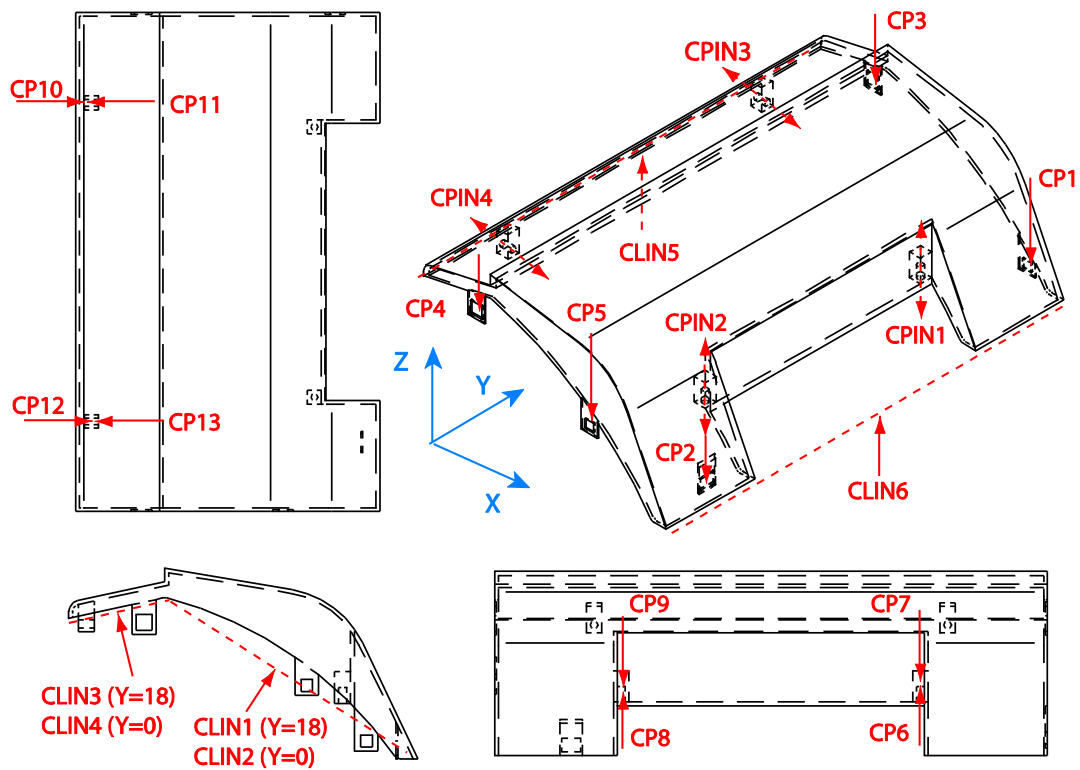
Figure 10.11 Printer housing geometry and assembly constraints

	P_x	P_y	P_z	N_x	N_y	N_z
CP1	9.375	18.000	0.377	0.000	0.000	-1.000
CP2	10.299	2.500	0.125	0.000	0.000	-1.000
CP3	2.375	18.000	4.045	0.000	0.000	-1.000
CP4	2.375	0.000	4.045	0.000	0.000	-1.000
CP5	7.500	0.000	2.125	0.000	0.000	-1.000
CP6	8.625	13.875	1.744	0.000	0.000	1.000
CP7	8.625	13.875	1.744	0.000	0.000	-1.000
CP8	8.625	4.125	1.744	0.000	0.000	1.000
CP9	8.625	4.125	1.744	0.000	0.000	-1.000
CP10	0.322	14.750	4.250	1.000	0.000	0.000
CP11	0.322	14.750	4.250	-1.000	0.000	0.000
CP12	0.322	3.250	4.250	1.000	0.000	0.000
CP13	0.322	3.250	4.250	-1.000	0.000	0.000

	P_x	P_y	P_z	w_x	w_y	w_z
CPIN1	8.625	13.875	1.744	0.000	0.000	1.000
CPIN2	8.625	4.125	1.744	0.000	0.000	1.000
CPIN3	0.322	14.750	4.250	1.000	0.000	0.000
CPIN4	0.322	3.250	4.250	1.000	0.000	0.000

	P_x	P_y	P_z	w_x	w_y	w_z	N_x	N_y	N_z	L
CLIN1	7.125	18.000	3.200	-0.669	0.000	0.744	0.744	0.000	0.669	8.941
CLIN2	7.125	0.000	3.200	-0.669	0.000	0.744	0.744	0.000	0.669	8.941
CLIN3	1.551	18.000	4.754	0.978	0.000	0.211	-0.211	0.000	0.978	3.000
CLIN4	1.551	0.000	4.754	0.978	0.000	0.211	-0.211	0.000	0.978	3.000
CLIN5	0.000	9.000	4.420	0.000	1.000	0.000	0.000	0.000	1.000	11.500
CLIN6	11.000	9.000	0.000	0.000	1.000	0.000	0.000	0.000	1.000	18.000

Table 10.16 Printer housing constraint configuration

Each threaded fastener is modeled as a pin constraint with two unilateral point constraints along the fastener's axis with opposite directions. The pin constraint is due to the fastener's pin geometry, and the two-way point constraints are due to the thread in the fastener.

The perimeter edges have ribs that prevent motion in the XY plane; however, since the stiffness of the lip in this direction is must less than the unilateral constraint in the z-direction, they are neglected in the model. This is an important modeling guideline. There are features in the assembly that do not necessarily serve as constraints that remove DOF. In this case, the edge ribs/fingers serve an aesthetic function. The edge constraints force the lip of the housing and the mating part to deflect together without showing gaps. This is important for product handling because the plastic housing is flexible enough to cause these deflections, but they cannot act as effective mechanical constraints. Therefore, they are not shown in the figures for the reasons given above.

The higher order contacts that need to be considered to be modeled as HOC in this case are the line constraints along the perimeter of the housing. The lengths of line contacts modeled by CLIN1, CLIN2, CLIN5, and CLIN6 are almost equal to the part length and can readily be modeled as line constraints. Line contacts CLIN3 and CLIN4, however, are somewhat shorter than the others and slightly less than half of the overall part length in the same direction. Since CLIN3 and CLIN4 are not linearly dependent to another constraint, these lines are modeled as line constraints although they are relatively shorter.

10.5.1 Baseline analysis results

Table 10.17 shows the analysis results.

Overall Rating Metric		
Weakest Total Resistance rating (WTR)	2.437	(LAR: 0.410)
Mean Redundancy Ratio (MRR)	4.555	
Mean Total Resistance Rating (MTR)	17.628	(LAR: 0.057)
Trade Off Ratio (TOR)	3.870	

	Screw axis direction (ω)			Screw axis coincident point (ρ)			Pitch (h)	Total Resistance Rating
WTR Motion 1	0.000	0.000	-1.000	0.322	3.250	0.000	0.000	*2.437*
WTR Motion 2	0.000	0.000	-1.000	0.322	0.000	0.000	0.000	*2.438*
WTR Motion 3	0.000	0.000	1.000	0.323	14.756	0.000	0.000	*2.437*
WTR Motion 4	0.000	0.000	1.000	0.323	17.987	0.000	0.000	*2.439*

	Active %	Best Resistance %		Active %	Best Resistance %
CP1	27.2%	2.3%	CPIN1	38.7%	1.5%
CP2	26.0%	1.5%	CPIN2	38.7%	0.9%
CP3	27.2%	2.9%	CPIN3	63.6%	6.4%
CP4	27.2%	2.3%	CPIN4	63.6%	2.9%
CP5	27.2%	0.3%			
CP6	23.7%	0.0%	CLIN1	45.4%	7.8%
CP7	23.7%	0.0%	CLIN2	47.4%	6.9%
CP8	23.7%	0.0%	CLIN3	40.5%	8.1%
CP9	23.7%	0.0%	CLIN4	39.9%	7.2%
CP10	17.9%	0.0%	CLIN5	39.0%	5.8%
CP11	17.9%	5.5%	CLIN6	49.7%	5.5%
CP12	17.9%	0.0%			
CP13	17.9%	5.2%			

Table 10.17 Printer housing baseline analysis results

The baseline analysis result shows that the assembly is in general more redundant than the previous case studies. The MRR value of 4.513 means that on average the total resistance value is 4.513 times the best resistance offered by the most effective constraint.

Redundant designs usually result in higher MTR value. The MTR value of 12.734, or an equivalent load amplification ratio of 0.079, shows that each constraint only carries less than 1/10 of the input load on average. This design is capable of handling large loads due to its redundancy.

A quick observation on the individual constraint's active and best resistance percentage shows that the resistance is fairly well distributed. Although the higher order constraints such as the pin and line constraints generally are more active, the point constraints' activity is not negligible.
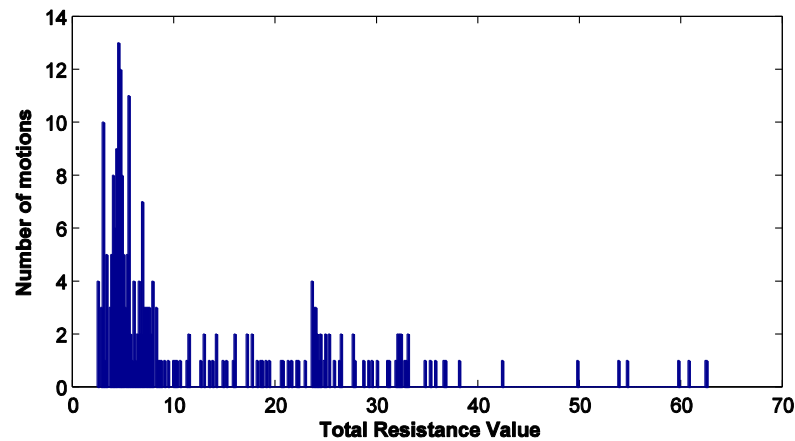

Figure 10.12 Total resistance histogram for printer housing assembly

The total resistance histogram (Figure 10.12) shows that the distribution is skewed to the left, which means that although the average total resistance (MTR) is 12.73, the majority of the motions are rated below 8.0. The symmetry in this part is less compared to the previous case studies, hence, less symmetry is observed in the evaluated motion set. Most symmetrical motions with symmetrical reaction constraints are usually

rated identically. This is not shown to be dominant in the histogram as the motion ratings are more randomly rather than uniformly distributed.

10.5.2 Snap-fits vs. threaded fasteners

If the snap-fits in the printer housing assembly are replaced by all threaded fasteners, the MRR increases by 84% (Table 10.18). Although a significant resistance quality gain is obtained (81%), the redundancy increase might be unacceptable because it leads to more internal stresses. This trade-off will be explored further in the next chapter.

	Design with 4 locating pins and 5 snap-fits	Design with 9 threaded fasteners	% Difference
WTR	1.578	4.481	184.0%
MRR	3.5283	6.494	84.0%
MTR	14.8045	26.757	80.7%
TOR	4.1959	4.121	-1.8%

Table 10.18 Comparison between snap-fit and threaded fasteners